

# Structure of arsenic-treated indium phosphide (001) surfaces during metalorganic vapor-phase epitaxy

D. C. Law, Y. Sun, C. H. Li, S. B. Visbeck, G. Chen, and R. F. Hicks\*

*Department of Chemical Engineering, University of California, Los Angeles, California 90095*

(Received 4 February 2002; published 22 July 2002)

We have studied the initial stages of heterojunction formation during the metalorganic vapor-phase epitaxy of indium arsenide on indium phosphide. Exposing an InP (001) film to 10 mTorr of tertiarybutylarsine below 500 °C results in the deposition of a thin InAs layer from 1.5 to 5.0 atomic layers thick (2.3–7.5 Å). The surface of this epilayer remains atomically smooth independent of arsenic exposure time. However, in an overpressure of tertiarybutylarsine at or above 500 °C, the arsenic atoms diffuse into the bulk, creating strained InAsP films. These films form three-dimensional island structures to relieve the built-up strain. The activation energy and pre-exponential factor for arsenic diffusion into indium phosphide have been determined to be  $E_d = 1.7 \pm 0.2$  eV and  $D_o = 2.3 \pm 1.0 \times 10^{-7}$  cm<sup>2</sup>/s.

DOI: 10.1103/PhysRevB.66.045314

PACS number(s): 68.35.Bs, 68.35.Dv, 68.35.Fx, 68.35.Ct

## INTRODUCTION

Compound semiconductors and their alloys are the key materials for high-speed electronic and optoelectronic devices, such as heterojunction bipolar transistors, lasers, and photodetectors.<sup>1–3</sup> Indium phosphide materials have gained interest recently due to their application in high-frequency devices used for fiber-optic communication.<sup>4–6</sup> These optoelectronic devices consist of alternating thin films of lattice-matched InGaAs, InGaAsP, and InP.<sup>3,4,7</sup> The interface structure between the alloy layers and indium phosphide have a direct impact on device performance.<sup>2,6,8–10</sup> In particular, the interfacial layers may contain defects and exhibit composition gradients that reduce electron mobility, enhance nonradiative carrier recombination, or alter quantum confinement energies.<sup>8,11</sup> Thus, in order to fabricate high-performance devices, one must control the interface structure on the atomic scale.

Metalorganic vapor-phase epitaxy (MOVPE) is widely used to fabricate InP-based materials.<sup>2</sup> During the growth of heterojunctions, e.g., InGaAs on InP, the group-V source must be switched from phosphorus to arsenic. However, simultaneous adsorption, desorption, and bulk diffusion of arsenic and phosphorus atoms have made it challenging to fabricate atomically abrupt interfaces.<sup>2,3</sup> Switching procedures with growth interruptions have been implemented in an attempt to solve this problem. This has led to many studies that focus on the effect of precursor switching procedures on material quality and device properties.<sup>1,2,6,12–14</sup> Most switching sequences consist of a hydrogen annealing step,  $t_1$ , a brief exposure to arsine,  $t_2$ , and then addition of the group-III precursors. This sequence is illustrated in Fig. 1. The flowing H<sub>2</sub> gas sweeps any remaining phosphine out of the MOVPE reactor, so that no phosphorus is incorporated into subsequently deposited layers. Introduction of arsine or tertiarybutylarsine prior to the group-III precursors ensures that the surface is group-V rich and prevents the formation of metal droplets at the onset of film growth. However, little is known about the evolution of the semiconductor surface structure during the hydrogen and arsine exposure steps.

In this work, we have characterized the initial stages of InGaAs/InP heterojunction formation during MOVPE growth by x-ray photoelectron spectroscopy (XPS), low-energy electron diffraction (LEED), and scanning tunneling microscopy (STM). The surface roughness, atomic structure, and composition of the indium phosphide films during growth interruptions,  $t_1$  and  $t_2$ , have been determined as a function of temperature and time. We find that arsenic atoms incorporate into only the top two to three bilayers of indium phosphide below 500 °C, whereas at or above 500 °C, they diffuse into the bulk crystal as well.

## EXPERIMENTAL METHODS

Indium phosphide films, 0.20 μm thick, were grown on *n*-type vicinal InP (001) substrates in a horizontal MOVPE reactor.<sup>15</sup> The growth temperature and total reactor pressure were 535 °C and 20 Torr. Hydrogen carrier gas was passed through a SAES Pure Gas H<sub>2</sub> purifier (PS4-MT3-H) to remove oxygen, nitrogen, water, and other impurities. Trimethylindium (TMIn) and tertiarybutylphosphine (TBP) were used to deposit the films with partial pressures of  $6.5 \times 10^{-4}$  and  $1.3 \times 10^{-1}$  Torr, respectively. After deposition, the InP crystals were heated in flowing hydrogen at 500 °C for up to 20 min creating an In-rich surface. The samples were then either transferred directly to the UHV system for surface analysis, or remained in the reactor for TBAs exposure.

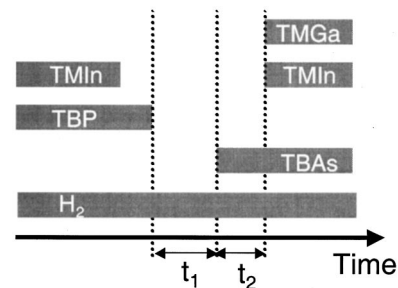


FIG. 1. Schematic of the precursor switching sequence during the growth of an InGaAs/InP heterojunction by MOVPE.

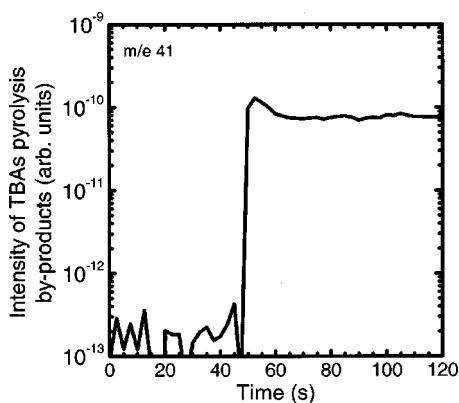


FIG. 2. The mass spectrometer response to a reaction by-product, propylene, during the introduction of tertiarybutylarsine to the MOVPE reactor.

Arsenic was introduced to the indium phosphide surface by exposing the crystal to 10.0 mTorr of tertiarybutylarsine at 350–600 °C for 5–600 s. A mass spectrometer was attached to the exhaust of the MOVPE reactor to monitor the arsenic exposure in real time.<sup>16</sup> Figure 2 shows the instantaneous increase in concentration of pyrolysis by-products (in this case, propylene) when TBAs was introduced into the reactor. After the exposure, the samples were cooled to 30 °C in an H<sub>2</sub> ambient at a rate of 4 °C/s.

Periodically during the TBAs exposure, the indium phosphide samples were analyzed by XPS, LEED, and STM. Core-level photoemission spectra of the As 3*d*, P 2*p*, and In 3*d* lines were collected by a PHI 3057 XPS spectrometer, using aluminum K<sub>α</sub> x-rays ( $h\nu=1486.6$  eV). The binding energies of the As 3*d*, P 2*p*, and In 3*d* levels are 41.5, 133.0, and 444.0 eV, respectively.<sup>17</sup> The As 3*d* and P 2*p* photoelectrons exhibit the same inelastic mean free path of ~25 Å.<sup>18,19</sup> All XPS spectra were taken in small area mode with a 7° acceptance angle and 23.5-eV pass energy. The take-off angle with respect to the surface normal was 25°.

The indium phosphide surface structure was characterized using a Princeton Instruments low-energy electron diffractometer. In addition, filled-states scanning tunneling micrographs were obtained with a Park Scientific Instruments AutoProbe VP at a bias of -3.6 V and a tunneling current of 1.0 nA. Images were acquired on different areas of each sample for comparison. Height data were acquired from the STM images at a resolution of 256×256 pixels. These data were used to calculate the root-mean-square (rms) surface roughness:

$$R_q = \sqrt{\frac{1}{N} \sum [h(x,y) - \bar{h}]^2}, \quad (1)$$

where  $h(x,y)$  is the surface height at location  $(x,y)$ ,  $\bar{h}$  is the average surface height, and  $N$  is the total number of data points.

## RESULTS

In Fig. 3, the phosphorus coverage on the indium phosphide (001) surface is plotted against the hydrogen annealing

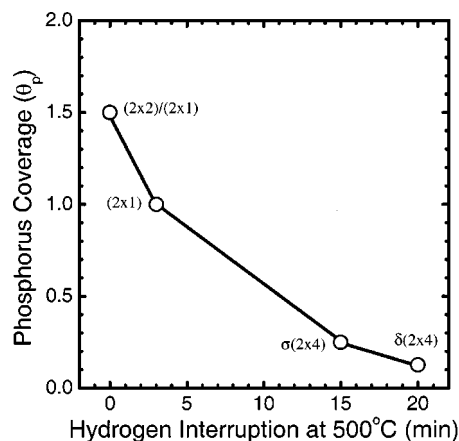


FIG. 3. The dependence of the phosphorus coverage on time during exposure of the InP (001) surface to 20 Torr hydrogen at 500 °C.

time at 500 °C. The coverage is assessed from LEED patterns and STM images, which correspond to known surface structures as described in the following paragraph. The as-grown InP film is terminated with 1.5 monolayers (ML's) of P atoms. Annealing for 3, 15, and 20 min decreases the phosphorus coverage to 1.0, 0.25, and finally 0.125 ML's, respectively. Holding the InP film for longer times in flowing H<sub>2</sub> results in surface degradation and indium droplet formation.

Hicks and co-workers have determined the surface structure of InP (001) as a function of the phosphorus coverage.<sup>20–22</sup> At  $\theta_p=1.5$  ML's, a  $(2 \times 2)/(2 \times 1)$  reconstruction is observed that consists of half a monolayer of phosphorus dimers adsorbed on top of a complete layer of P atoms. Desorbing the excess phosphorus yields a pure  $(2 \times 1)$  phase with  $\theta_p=1.0$  ML. The  $(2 \times 1)$  is covered with a complete layer of buckled phosphorus dimers, which are revealed in STM images as zigzagging rows of gray spots.<sup>21</sup> At  $\theta_p=0.25$  ML, an indium-rich  $\sigma(2 \times 4)$  reconstruction is recorded. The unit cell of this structure contains a single phosphorus dimer sitting astride four indium dimers. As observed in the STM, the P dimers from adjacent unit cells line up in straight rows extending along the  $[\bar{1}10]$  direction. At a slightly lower P coverage of 0.125 ML, the  $\delta(2 \times 4)$  phase is observed. This structure is the same as the  $\sigma(2 \times 4)$  except that the P-P dimer in the top layer is replaced with a mixed In-P dimer.<sup>22</sup>

The indium phosphide surface remains atomically smooth during the phase transition from a P-rich to an In-rich surface. Figure 4 shows an STM micrograph of the In-rich surface obtained after annealing in 20 Torr flowing H<sub>2</sub> for 20 min at 500 °C. The surface exhibits atomically flat terraces with an rms roughness of 1.1 Å. A sharp  $(2 \times 4)$  LEED pattern is recorded for this sample. In addition, the reflectance difference spectrum is indicative of a  $\delta(2 \times 4)$  reconstruction with the In-P and In-In dimer termination.<sup>23,24</sup>

Indium-rich  $(2 \times 4)$  surfaces with phosphorus coverages of about 0.2 ML were exposed to tertiarybutylarsine in the MOVPE reactor. The dependence of the arsenic atomic percentage on the exposure time and temperature is shown in Fig. 5. The As at. % was determined from the integrated



FIG. 4. Scanning tunneling micrograph of the InP (001) surface after a 20-min  $H_2$  anneal in the MOVPE reactor at 500 °C (image size =  $0.15 \times 0.15 \mu m^2$ ).

intensity of the 3d photoemission peak. The percentage represents the arsenic composition averaged over the electron mean free path, which is the top 25 Å of the film. A rapid uptake of arsenic is recorded over the first 10 s, followed by a much more gradual increase over 20–600 s. From 350 to 450 °C, the uptake appears to saturate at long times, whereas from 500 to 600 °C, the amount of arsenic in the near surface region is still increasing after a 600-s treatment in TBAs. Furthermore, the As content of the film measured after 100 s goes up with increasing exposure temperature. For example, at 350, 400, and 450 °C, the amount of arsenic at saturation is 15, 18, and 20 at. %, respectively.

The surface roughness of the indium phosphide films after 300 s of TBAs exposure is plotted as a function of temperature in Fig. 6. The surfaces are extremely smooth up to 500 °C, exhibiting an average rms roughness of 1.4 Å. However, the  $R_q$  jumps to 9.5 and 20.0 Å for treatments at 550 and 600 °C. As noted above, there is a continuous slow up-

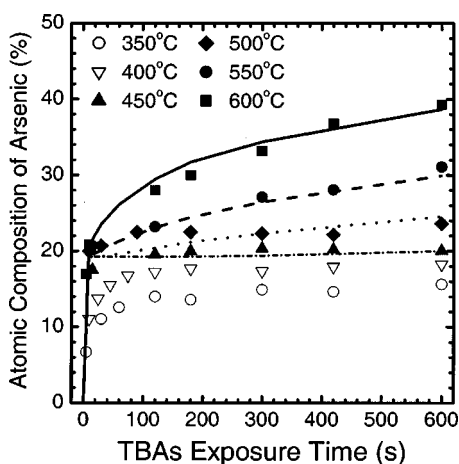


FIG. 5. The dependence of the arsenic content in the near-surface region on the time and temperature of exposure to 10.0 mTorr TBAs [symbols: experimental data; lines: fit of the data to Eq. (11)].

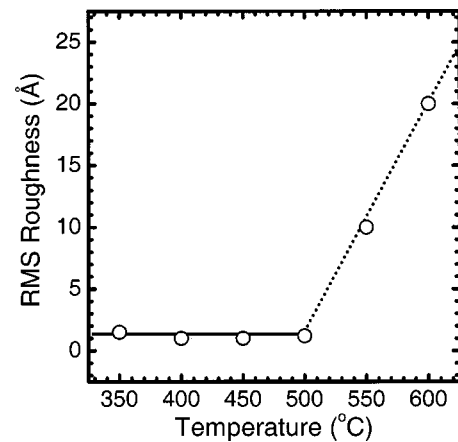


FIG. 6. The dependence of the rms surface roughness on the temperature of exposure to 10.0 mTorr TBAs for 300 s in the MOVPE reactor.

take of arsenic at these higher temperatures.

Figure 7 displays an STM picture of the InP film after annealing it in tertiarybutylarsine at 350 °C. Initially, the surface exhibited an indium-rich ( $2 \times 4$ ) LEED pattern, whereas after the TBAs exposure, a weak ( $2 \times 1$ ) was recorded. Examination of the image reveals a random pattern of white and gray spots from 30 to 60 Å across and from 2.0 to 4.0 Å in height. These spots cover 85% of the surface. The inset picture shows a closeup of the surface after heating the sample to 300 °C in ultrahigh vacuum to desorb some of the arsenic. Below the white spots a series of uniform gray rows can be seen that extend in the  $[110]$  direction. These rows exhibit the zigzag pattern of the InP (001)-( $2 \times 1$ ) reconstruction.<sup>21,25</sup> The vertical distance from the ( $2 \times 1$ ) rows to the top of the white spots is one atomic layer. It is concluded that the gray and white spots are due to clusters of arsenic atoms adsorbed on top of a full monolayer of As and P atoms.

Presented in Fig. 8 is an STM micrograph of the InP film after exposing it to tertiarybutylarsine at 500 °C. A ( $2 \times 4$ ) LEED pattern is recorded before and after the treatment. The image exhibits a mottled white, gray, and black pattern due

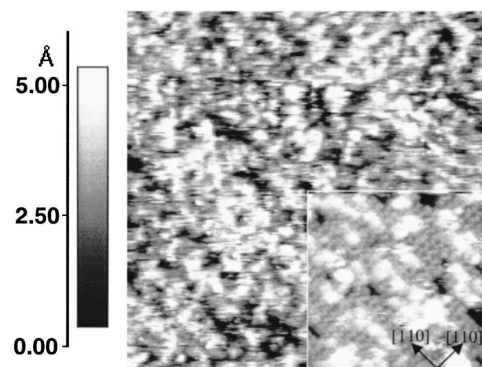


FIG. 7. Scanning tunneling micrograph of the As:InP (001) surface after exposure to 10.0 mTorr TBAs for 300 s at 350 °C (large image size =  $0.13 \times 0.13 \mu m^2$ ; inset image size =  $400 \times 400 \text{ \AA}^2$ ).

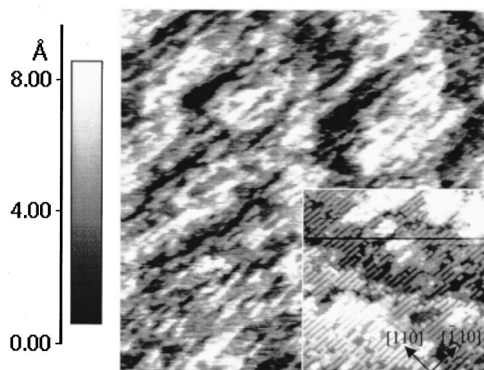


FIG. 8. Scanning tunneling micrograph of the As:InP (001) surface after exposure to 10.0 mTorr TBAs for 300 s at 500 °C (large image size= $0.13 \times 0.13 \mu\text{m}^2$ ; inset image size= $750 \times 750 \text{Å}^2$ ).

to two-dimensional islands that are elongated in the  $[\bar{1}10]$  direction. The black-to-white contrast encompasses only three bilayers of the crystal. This sample was annealed in ultrahigh vacuum at 300 °C for 15 min to remove any adsorbed carbon and other impurities. Then the magnified STM image shown in the inset was obtained. In this picture, one sees gray rows running parallel to the  $[\bar{1}10]$  axis. The row structure is characteristic of the  $(2 \times 4)$  reconstruction found on GaAs and InAs (001) surfaces.<sup>26–30</sup> Each  $(2 \times 4)$  unit cell consists of two As dimers separated by a trench that contains either two Ga dimers, or a third As dimer, yielding arsenic coverages of 0.5 and 0.75 ML. The surface structure seen in Fig. 8 is obtained following exposure to TBAs at temperatures up to 600 °C, provided that the annealing time is kept below 10 s.

In Fig. 9, a large-area STM micrograph of the InP film surface after treatment in tertiarybutylarsine for 300 s at 550 °C is presented. No LEED pattern was discernable for this sample. The original flat terraces (cf. Fig. 4) are no longer present. Instead, they have been replaced by three-dimensional islands whose width varies between 100 and 250 Å and height ranges from 30 to 75 Å. Some of the islands have coalesced into larger structures as seen on the

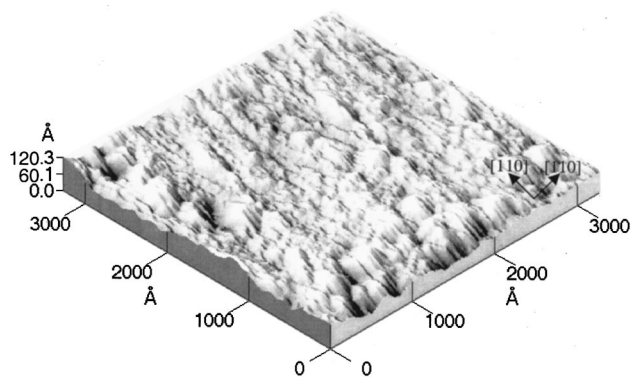


FIG. 9. Scanning tunneling micrograph of the As:InP (001) surface after exposure to 10.0 mTorr TBAs for 300 s at 550 °C (image size= $0.30 \times 0.30 \mu\text{m}^2$ ).

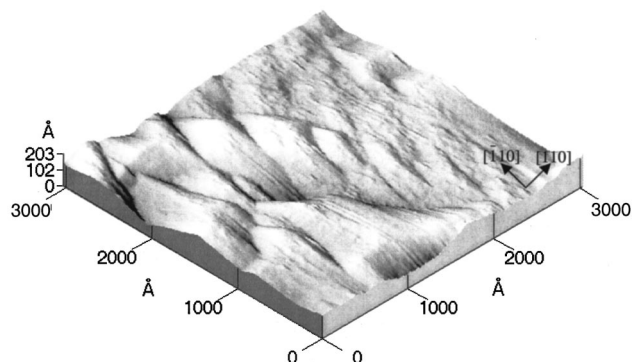


FIG. 10. Scanning tunneling micrograph of the As:InP (001) surface after exposure to 10.0 mTorr TBAs for 600 s at 550 °C (image size= $0.32 \times 0.32 \mu\text{m}^2$ ).

right side of the picture. The random pattern of the islands made it impossible to obtain atomic-scale images of the surface.

An STM picture of the InP surface after exposure to tertiarybutylarsine for 600 s at 550 °C is shown in Fig. 10. Much larger islands are observed than those recorded following the 300-s treatment. The islands average approximately 1000 Å in width by 150 Å in height. Also evident are ridges and valleys crisscrossing the surface. This large-scale roughening of the surface corresponds with the continuous gradual uptake of arsenic at long exposure times, as recorded in Fig. 5.

## DISCUSSION

### Hydrogen interrupt

During the hydrogen interrupt,  $t_1$ , in the MOVPE reactor at  $\geq 500$  °C, the amount of phosphorus on the InP surface decreases from about 1.5 to 0.125 ML. Phosphorus desorption occurs with a smooth transition in the surface reconstruction from  $(2 \times 2)/(2 \times 1)$  to pure  $(2 \times 1)$  to  $\sigma(2 \times 4)$  and to  $\delta(2 \times 4)$ . Throughout this process, the RMS roughness remains constant at 1.1 Å. However, if the growth interrupt proceeds for too long in time, indium droplets can form which may destroy the sample. Our findings agree with previous studies of this phenomenon, in which the InP film was monitored *in situ* by reflectance difference spectroscopy.<sup>31</sup> During  $\text{H}_2$  annealing, the optical spectra indicated that the surface undergoes a rapid transition from a P-rich to In-rich reconstruction without any roughening. At 625 °C, this transition occurred in 1 s.<sup>32</sup> It should be recognized that the exact process parameters needed to achieve a given phosphorus coverage depend on the temperature, total pressure, hydrogen flow rate, and individual reactor design.

### Low-temperature TBAs exposure

At 350 to 450 °C, the adsorption of tertiarybutylphosphine on the indium-rich InP (001) surface follows Langmuir-like behavior. The arsenic content rises rapidly at first and then levels off to a constant value independent of time. The LEED and STM results indicate that the saturation coverage of group-V elements decreases with increasing temperature:

$\theta_P \sim 1.5$  ML's at 350 °C, while  $\theta_P \sim 0.75$  ML at 450 °C. By contrast, the XPS data show that the amount of arsenic in the near-surface region increases with increasing temperature: 15% at 350 °C vs 20% at 450 °C. These findings lead us to conclude that at the higher growth temperature, the As atoms replace the P atoms in the first two to three bilayers of the crystal. In other words, a coherently strained indium arsenide film, about 7.5 Å thick, is deposited on the indium phosphide during exposure to TBAs at 450 °C. Once this thin film has formed no further adsorption takes place. This is in agreement with previous work that found evidence for the formation of a sharp, two-dimensional InAs/InP interface at 400–520 °C.<sup>8,9</sup>

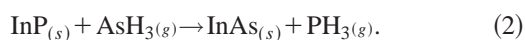
Li *et al.*<sup>25</sup> have identified the surface structures obtained after arsenic adsorption and exchange with phosphorus on indium phosphide under ultrahigh vacuum conditions. The reconstructions observed here are analogous to those seen in UHV. At about 300 °C, tertiarybutylarsine decomposes on the indium-rich InP (001) surface and deposits more than one monolayer of As atoms, generating a disordered (1×4) phase. This structure consists of small clusters of As dimers adsorbed on top of a complete layer of As+P atoms; much like that seen in the STM images presented in Fig. 7. At temperatures ranging from 350 to 400 °C, phosphorus desorption accompanies arsenic adsorption, with the As atoms exchanging into the group-V sites in the top three bilayers of the crystal. Two types of reconstructions are seen on these InAs/InP heterostructures: the  $\beta 2(2 \times 4)$  and  $\alpha 2(2 \times 4)$  with 2-As dimers exposed on the surface.

### High-temperature TBAs exposure

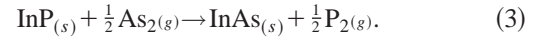
Arsenic incorporation occurs in two stages when the indium phosphide is exposed to tertiarybutylphosphine above 500 °C. In about 10 s, the As atoms exchange with the P atoms in the first 7.5 Å of the crystal, forming an ultrathin InAs film. Then with increasing exposure time, the arsenic slowly migrates into the bulk InP. This generates a thick InAsP film, which is highly strained due to the large lattice mismatch with the substrate (3.2% between InAs and InP). To relieve this strain, the film reorganizes into three-dimensional islands as seen in the two STM images presented in Figs. 9 and 10.<sup>33</sup>

Our results agree with previous studies of indium gallium arsenide deposition on indium phosphide.<sup>32,34–36</sup> Sudo *et al.*<sup>32</sup> observed that during a TBAs growth interrupt ( $t_2$ ) at 650 °C, the ellipsometer signal stayed constant for a few seconds, then gradually drifted upwards with longer exposure time.<sup>32</sup> The signal shift was due to surface roughening that the authors believed was caused by three-dimensional island formation. Several other researchers have reported that islands are produced when InP is exposed to arsine above 500 °C in an MOVPE reactor.<sup>35–37</sup>

Arsenic exchange for phosphorus can follow two different pathways.<sup>8</sup> In one case, arsine may react with the surface generating indium arsenide and phosphine:



Alternatively, arsenic dimers present in the gas may displace adsorbed phosphorus dimers:



The standard heats of reaction of Eqs. (2) and (3) are calculated to be  $-29.0$  and  $4.5$  kJ/mol at 500 °C. In addition, the Gibbs free energies of reaction ( $\Delta G_{rxn}$ ) at 500 °C equal  $-31.5$  and  $-3.5$  kJ/mol, respectively. The heats of formation, entropies and heat capacities of InP, InAs, P<sub>2</sub>, PH<sub>3</sub>, As<sub>2</sub>, and AsH<sub>3</sub> have been obtained from published thermodynamic data.<sup>7,38–40</sup> Although we have not been able to find thermodynamic data for TBAs and TBP, these organometallic sources are expected to behave similarly to their MH<sub>3</sub> counterparts. The negative values of  $\Delta G_{rxn}$  imply that reactions (2) and (3) are thermodynamically favorable at 500 °C, in agreement with this work and other studies of arsenic exchange with the InP surface.<sup>35,36,41,42</sup>

It is proposed that the arsenic atoms incorporate into the indium phosphide crystal via a Frank-Turnbull mechanism involving phosphorus vacancies:<sup>4</sup>



where  $i_{\text{As}}$  represents an arsenic atom at an interstitial site,  $V_{\text{P}}$  is a phosphorus vacancy, and  $\text{As}_{\text{P}}$  is an arsenic atom occupying a phosphorus lattice site. Phosphorus desorption above 350 °C creates vacancies near the InP surface.<sup>37,43</sup> These migrate into the bulk as anions move upward to fill these sites.<sup>44,45</sup> Upon exposure to an overpressure of tertiarybutylarsine, arsine, or arsenic above 500 °C, As atoms can be driven into the bulk to fill the vacant group-V sites. A similar mechanism has been observed for phosphorus diffusion in gallium arsenide below 900 °C.<sup>46</sup>

A differential mass balance for arsenic diffusion into indium phosphide is given by

$$\frac{\partial N_{\text{As}}}{\partial t} = D_{\text{eff}}^{\text{As}} \frac{\partial^2 N_{\text{As}}}{\partial x^2}. \quad (5)$$

Here,  $N_{\text{As}}$  is the arsenic concentration (atoms/cm<sup>3</sup>),  $D_{\text{eff}}^{\text{As}}$  is the effective diffusivity of arsenic (cm<sup>2</sup>/s),  $t$  is time (s), and  $x$  is distance (cm). The effective diffusivity depends on temperature according to the Arrhenius relationship,

$$D_{\text{eff}}^{\text{As}} = D_o \exp\left(\frac{-E_d}{k_B T}\right), \quad (6)$$

where  $E_d$  and  $D_o$  are the activation energy (eV) and pre-exponential factor (cm<sup>2</sup>/s) for As diffusion, and  $k_B$  is Boltzmann's constant (eV/K). As discussed above, the surface of the InP film is immediately replaced with a 7.5-Å-thick InAs layer upon exposure to tertiarybutylarsine. Consequently, the initial and boundary conditions correspond to a constant-source diffusion model where the solution to Eq. (6) is given by the complementary error function,<sup>47</sup>

$$N_{\text{As}} = 0.5N_T \operatorname{erfc} \frac{x}{2\sqrt{D_{\text{eff}}^{\text{As}} t}}, \quad (7)$$

with  $N_T$  equal to the total atomic density of the InAs film (atoms/cm<sup>3</sup>).

The XPS data presented in Fig. 5 document the diffusion of arsenic into the bulk at temperatures  $\geq 500$  °C, since the As 3*d* emission intensity arises from atoms dispersed over the first eight bilayers of the film, i.e., 25 Å. However, folded into the measured intensity is the concentration profile given by Eq. (7) and the scattering of the photoelectrons by the crystal lattice. This latter process may be described by the following equation:<sup>48,49</sup>

$$I_{As} = \exp\left(\frac{-x}{\lambda_{As} \cdot \cos(\alpha)}\right), \quad (8)$$

where  $I_{As}$  is the normalized As 3*d* peak intensity for an InAs surface,  $\lambda_{As}$  is the electron inelastic mean free path, 25 Å, and  $\alpha$  is the take-off angle, 25°. In Eq. (8) it is assumed that the photoelectrons are being ejected from a thick indium arsenide film. However, in the present case, arsenic has been substituted for phosphorus in indium phosphide, and the depth-dependent intensity must be multiplied by the fraction of group-V sites occupied with As atoms, i.e.,

$$I_{As/InP} = (2N_{As}/N_T) \cdot I_{As}. \quad (9)$$

Similarly, for the normalized intensity of the P 2*p* photoemission line,

$$I_{P/InP} = (2N_P/N_T) \cdot \exp\left(\frac{-x}{\lambda_P \cdot \cos(\alpha)}\right). \quad (10)$$

Here,  $N_P$  is the phosphorus concentration (atoms/cm<sup>3</sup>) and  $\lambda_P$  is the inelastic mean free path of the P 2*p* photoelectrons. Note that  $\lambda_P = \lambda_{As} = 25$  Å,<sup>18,19</sup> which is consistent with the observation that the As and P atomic percentages always sum to  $50 \pm 5\%$ , irrespective of the arsenic uptake.

The measured intensity of the arsenic and phosphorus lines is obtained by integrating Eqs. (9) and (10) over distance. To calculate the arsenic atomic percentage, the As peak intensity must be divided by two times the sum of the As and P peak intensities. Thus, by combining Eqs. (8), (9), and (10), and integrating them, we have

$$\text{As(atom\%)} = \frac{\int_0^\infty N_{As} \cdot \exp\left(\frac{-x}{\lambda_{As} \cdot \cos(\alpha)}\right) \cdot dx}{N_T \int_0^\infty \exp\left(\frac{-x}{\lambda_{As} \cdot \cos(\alpha)}\right) \cdot dx}. \quad (11)$$

This equation has been solved by summing the expressions inside the integrands over the first 20 atomic layers of the film. To account for the top 7.5 Å of indium arsenide and the corresponding surface structure, the values of  $N_{As}$  in the first, third, and fifth atomic layers were set equal to 0.5, 1.0, and

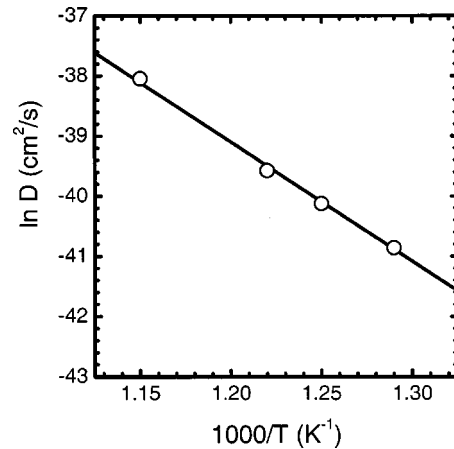


FIG. 11. The dependence of the arsenic diffusivity in indium phosphide on the inverse temperature.

$1.0 N_T$ . This yielded an As content of 20 at. % for the ultrathin InAs film. For odd atomic layers below the fifth one,  $N_{As}$  was calculated from Eq. (7).

The effective diffusion coefficient has been determined by obtaining the best fit of Eq. (11) to the data presented in Fig. 5. The dotted, dashed, and solid lines in the figure represent the fits at 500, 550, and 600 °C, respectively. The values obtained for  $D_{\text{eff}}^{As}$  are presented in Fig. 11 as a function of the inverse temperature. The activation barrier and pre-exponential factor are estimated to be  $1.7 \pm 0.2$  eV and  $2.3 \pm 1.0 \times 10^{-7}$  cm<sup>2</sup>/s. Our results agree with those of Gillin and co-workers,<sup>3</sup> who measured a 1.7 eV activation energy for arsenic interdiffusion in InGaAsP alloys.

## CONCLUSIONS

We have characterized the initial stages of heterojunction formation in metalorganic vapor-phase epitaxy of indium arsenide on indium phosphide. The hydrogen growth interrupt,  $t_1$ , and the arsenic growth interrupt,  $t_2$ , have a strong impact on the composition and structure of the interface. During tertiarybutylarsine exposure below 500 °C, arsenic atoms adsorb and replace the phosphorus atoms in the first three bilayers of the crystal, generating an ultrathin InAs film. Conversely, during TBAs exposures of 10 s or more above 500 °C, arsenic atoms diffuse into the bulk crystal, creating strained indium arsenide phosphide films that transform into a three-dimensional island structure.

## ACKNOWLEDGMENTS

Funding for this research was provided by the National Science Foundation, Divisions of Chemical and Transport Systems and Materials Research, and by the California Energy Innovations Small Grant Program.

\*Author to whom correspondence should be addressed. Electronic address: rhicks@ucla.edu

<sup>1</sup>A. Y. Lew, C. H. Yan, R. B. Welstand, J. T. Zhu, C. W. Tu, P. K. L. Yu, and E. T. Yu, *J. Electron. Mater.* **26**, 64 (1997).

<sup>2</sup>T. Nakamura, S. Ae, T. Terakado, T. Torikai, and T. Uji, *J. Elec-*

*tron. Mater.* **25**, 457 (1996).

<sup>3</sup>W. P. Gillin, S. S. Rao, I. V. Bradley, K. P. Homewood, A. D. Smith, and B. A. T. R., *Appl. Phys. Lett.* **63**, 797 (1993).

<sup>4</sup>S. L. Wong, R. J. Nicholas, R. W. Martin, J. Thompson, A. Wood, A. Moseley, and N. Carr, *J. Appl. Phys.* **79**, 6826 (1996).

- <sup>5</sup>B. W. Liang and C. W. Tu, *J. Appl. Phys.* **74**, 255 (1993).
- <sup>6</sup>C. Lamberti, S. Bordiga, F. Boscherini, S. Mobilio, S. Pascarelli, L. Gastaldi, M. Madella, C. Papuzza, C. Rigo, D. Soldani, C. Ferrari, L. Lazzarini, and G. Salviati, *J. Appl. Phys.* **83**, 1058 (1998).
- <sup>7</sup>A. S. Jordan and A. Robertson, *J. Vac. Sci. Technol. A* **12**, 204 (1994).
- <sup>8</sup>T. Anan, S. Sugou, K. Nishi, and T. Ichihashi, *Appl. Phys. Lett.* **63**, 1047 (1993).
- <sup>9</sup>D. E. Aspnes, M. C. Tamargo, M. J. S. P. Brasil, R. E. Nahory, and S. A. Schwarz, *Appl. Phys. Lett.* **64**, 3279 (1994).
- <sup>10</sup>W. Wu, S. L. Skala, J. R. Tucker, J. W. Lyding, A. Seabaugh, E. A. Beam III, and D. Jovanovic, *J. Vac. Sci. Technol. A* **13**, 602 (1995).
- <sup>11</sup>A. Freundlich, M. F. Vilela, C. Monier, L. Aguilar, F. Newman, and I. Serdiukova, *Conference Record of the Twenty Sixth IEEE Photovoltaic Specialists Conference—1997* (Cat. No. 97CB36026).
- <sup>12</sup>M. Takemi, Y. Mihashi, T. Shiba, and M. Aiga, *J. Cryst. Growth* **191**, 18 (1998).
- <sup>13</sup>J. Hergeth, D. Grützmacher, F. Reinhardt, and P. Balk, *J. Cryst. Growth* **107**, 537 (1991).
- <sup>14</sup>J. Camassel, J. P. Laurenti, S. Juillaguet, F. Reinhardt, K. Wolter, H. Kurz, and D. Grützmacher, *J. Cryst. Growth* **107**, 543 (1991).
- <sup>15</sup>D. C. Law, L. Li, M. J. Begarney, and R. F. Hicks, *J. Appl. Phys.* **88**, 508 (2000).
- <sup>16</sup>M. J. Begarney, Ph.D. Dissertation, University of California, Los Angeles, 2001.
- <sup>17</sup>C. D. Wagner, W. M. Riggs, L. E. Davis, J. F. Moulder, and G. E. Muilenberg, *Handbook of X-ray Photoelectron Spectroscopy* (Perkin-Elmer Corporation, Norwalk, CT, 1979).
- <sup>18</sup>S. Tanuma, C. J. Powell, and D. R. Penn, *Acta Phys. Pol. A* **81**, 169 (1992).
- <sup>19</sup>G. Gergely, M. Menyhard, S. Gurban, Z. Benedek, C. Daroczi, V. Rakovics, J. Toth, D. Varga, M. Krawczyk, and A. Jablonski, *Surf. Interface Anal.* **30**, 195 (2000).
- <sup>20</sup>L. Li, B.-K. Han, D. Law, C. H. Li, Q. Fu, and R. F. Hicks, *Appl. Phys. Lett.* **75**, 683 (1999).
- <sup>21</sup>L. Li, B.-K. Han, Q. Fu, and R. F. Hicks, *Phys. Rev. Lett.* **82**, 1879 (1998).
- <sup>22</sup>L. Li, Q. Fu, C. H. Li, B.-K. Han, and R. F. Hicks, *Phys. Rev. B* **61**, 10 223 (2000).
- <sup>23</sup>M. J. Begarney, C. H. Li, D. C. Law, S. B. Visbeck, Y. Sun, and R. F. Hicks, *Appl. Phys. Lett.* **78**, 55 (2001).
- <sup>24</sup>D. C. Law, Q. Fu, S. Visbeck, Y. Sun, and R. F. Hicks, *Surf. Sci.* **496**, 121 (2001).
- <sup>25</sup>C. H. Li, L. Li, D. C. Law, S. B. Visbeck, and R. F. Hicks, *Phys. Rev. B* (to be published).
- <sup>26</sup>L. Li, B. K. Han, and R. F. Hicks, *Appl. Phys. Lett.* **73**, 1239 (1998).
- <sup>27</sup>L. Li, B. K. Han, S. Gan, H. Qi, and R. F. Hicks, *Surf. Sci.* **398**, 386 (1998).
- <sup>28</sup>C. Ratsch, W. Barvosa-Carter, F. Gross, J. H. G. Owen, and J. J. Zinck, *Phys. Rev. B* **62**, R7719 (2000).
- <sup>29</sup>M. D. Pashley, *Phys. Rev. B* **40**, 10 481 (1989).
- <sup>30</sup>D. K. Biegelsen, R. D. Bringans, J. E. Northrup, and L.-E. Swartz, *Phys. Rev. B* **41**, 5701 (1990).
- <sup>31</sup>T. Hannappel, S. Visbeck, M. Zorn, J.-T. Zettler, and F. Willig, *J. Cryst. Growth* **221**, 124 (2000).
- <sup>32</sup>S. Sudo, Y. Nakano, M. Sugiyama, Y. Shimogaki, H. Komiyama, and K. Tada, *Thin Solid Films* **313–314**, 604 (1998).
- <sup>33</sup>K. N. Tu, J. W. Mayer, and L. C. Feldman, *Electronic Thin Film Science for Electrical Engineers and Materials Scientist* (Macmillan, New York, 1992).
- <sup>34</sup>S. Anand, C. F. Carlstrom, A. Patel, E. Niemi, B. Stalnacke, and G. Landgren, *Proc. SPIE* **3975**, 1033 (2000).
- <sup>35</sup>C. F. Carlstrom, S. Anand, E. Niemi, and G. Landgren, *Eleventh International Conference on Indium Phosphide and Related Materials (IPRM'99)* (Cat. No. 99CH36362), IEEE, (1999), p. 519.
- <sup>36</sup>B. Wang, F. Zhao, Y. Peng, Z. Jin, Y. Li, and S. Liu, *Appl. Phys. Lett.* **72**, 2433 (1998).
- <sup>37</sup>I. Rasnik, M. J. S. P. Brasil, F. Cerdeira, C. A. C. Mendonca, and M. A. Cotta, *J. Appl. Phys.* **87**, 1165 (2000).
- <sup>38</sup>D. R. Stull and G. C. Sinke, *Thermodynamic Properties of The Elements* (American Chemical Society, Washington DC, 1956).
- <sup>39</sup>K. Yamaguchi, Y. Takeda, K. Kameda, and K. Itagaki, *Mater. Trans., JIM* **35**, 596 (1994).
- <sup>40</sup>K. Yamaguchi, Y. Chiba, M. Yoshizawa, and K. Kameda, *J. Jpn. Inst. Met.* **60**, 1181 (1996).
- <sup>41</sup>L. G. Qualgiano, B. Jusserand, and D. Orani, *Phys. Rev. B* **56**, 4919 (1997).
- <sup>42</sup>M. Washima, T. Tsuchiya, T. Tani, and H. Sakaguchi, *Conference Proceedings, Seventh International Conference on Indium Phosphide and Related Materials.* (Cat. No. 95CH35720) **IEEE** (1995).
- <sup>43</sup>P. Ebert, M. Heinrich, M. Simon, K. Urban, and M. G. Lagally, *Phys. Rev. B* **51**, 9696 (1995).
- <sup>44</sup>M. Heinrich, P. Ebert, M. Simon, K. Urban, and M. G. Lagally, *J. Vac. Sci. Technol. A* **13**, 1714 (1995).
- <sup>45</sup>P. Juza, W. Faschinger, K. Hingerl, and H. Sitter, *Semicond. Sci. Technol.* **5**, 191 (1990).
- <sup>46</sup>R. F. Scholz and U. Gosele, *J. Appl. Phys.* **87**, 704 (2000).
- <sup>47</sup>R. C. Jaeger, *Introduction of Microelectronic Fabrication* (Addison-Wesley, Reading, MA, 1988).
- <sup>48</sup>Y. Feuprier, C. Cardinaud, and G. Turban, *J. Vac. Sci. Technol. B* **16**, 1823 (1998).
- <sup>49</sup>L. C. Feldman and J. W. Mayer, *Fundamentals of Surface and Thin Film Analysis* (Elsevier Science, New York, 1986).